Gas-solid two-phase turbulent flow in a circulating fluidized bed riser: an experimental and numerical study

Y. He[1,2], M. van Sint Annaland[1*], N.G. Deen[1], and J.A.M. Kuipers[1]
1, Department of Chemical Engineering, University of Twente, PO Box 217, 7500 AE Enschede, The Netherlands
2, Department of Power Engineering, College of Energy Science and Engineering, Harbin Institute of Technology, Harbin 150001, China

ABSTRACT

Hydrodynamics of gas-particle two-phase turbulent flow in a circulating fluidized bed riser is studied experimentally by Particle Image Velocimetry (PIV) and numerically with the use of a 3D discrete hard sphere particle model (DPM). Mean particle velocities and RMS velocities are obtained and the influence of turbulence on the flow is investigated. The experimental data are analyzed and compared with the numerical results showing a reasonable agreement.

KEYWORDS: Circulating fluidized bed riser, particle image velocimetry, discrete particle model, turbulence.

I. INTRODUCTION

Gas-solid fluidization using circulating fluidized beds (CFB) has found widespread application in industry, e.g. in fluid catalytic cracking (FCC) and CFB combustors. However, the behavior of complex flow structures emerging in this type of turbulent two-phase flow is still not fully understood, despite their importance on the overall reactor performance. Detailed experimental and numerical techniques are required to study the flow structures pertaining in CFB reactors in detail.

Some researchers have carried out experimental work to study the flow phenomena in circulating fluidized bed [2-6]. Most of them apply phase Doppler anemometry (PDA) or laser Doppler anemometry (LDA) to measure the flow characteristics in the riser. Laser Doppler anemometry (LDA) is a point measurement technique that is very well suited to measure the velocity and turbulence distribution in both free flows and internal flows at a high temporal resolution. Phase Doppler anemometry (PDA) is a similar technique that enables the simultaneous measurement of particle size, velocity and concentration. Particle image velocimetry (PIV) is a non-intrusive optical measurement technique using a laser light sheet and a CCD camera to investigate flow velocity structures. PIV enables the measurement of instantaneous whole field information of the flow structures, which is not possible with LDA or PDA.

Performing reliable measurements in CFB reactors is very difficult, since high volume fractions of particles prevent proper visual access to the measurement region. This is one of the reasons that numerical methods have become a popular alternative to study the hydrodynamics in circulating fluidized beds. Two theoretical approaches, Eulerian and the discrete particle (Lagrangian) approaches, were proposed to describe the complicated phenomena. Eulerian modeling considers the solid phases as well as the gas phase as continua where the presence of each phase is described by a phase volume fraction. Many researchers studied the multiphase flow in a riser, in which most adopt the Eulerian method to save computation time. The Eulerian model is able to predict the formation of clusters and describe the time-averaged solid concentration and flux distribution in circulating fluidized beds [7-10].

The Langrangian (discrete particle) approach includes hard-sphere and soft-sphere models as well as the DSMC (direct simulation Monte Carlo) method, in which the particle control volume is considered to move with the fluid [11-12]. Both the interactions between particles and between the particles and the gas phase are incorporated in this model. Contrary to the two-fluid model, the discrete particle model reveals the motion of individual particles. The DSMC method has relatively large computer memory requirements, so it can only deal with reactors of very small size. Due to the way the

* Corresponding author: email: M.vanSintAnnaland@utwente.nl; Tel.: +31 53 4894478; fax: +31 53 4892882

collisions are treated in the soft-sphere model, it is restricted to the use of very small time steps, which makes simulations with this model very time consuming. In this respect, the hard-sphere model seems most suited for simulations with a large number of particles. Due to the progress in computer hardware development, the DPM method becomes more and more popular in the computational research of fluidized beds. The advantage of the Lagrangian approach over Eulerian models is the fact that a more detailed model for the particle-particle interactions can be implemented.

In this work the hydrodynamics of gas-solid two-phase turbulent flow in a riser has been studied by detailed experiments using particle image velocimetry and detailed simulations with a 3D discrete particle model (DPM) in a well-defined geometry. In a pseudo two-dimensional circulating fluidized bed constructed of lexane (W × D × H = 0.015 m × 0.05 m × 1.5 m) spherical glass beads with a density of 2500 kg/m^3, an average diameter of 335 μm (250–420 μm) and an approximate shape factor of 1.0 were fluidized with air at a superficial gas velocity of 2.00 m/s and 2.30 m/s. The air was humidified up to a relative humidity of 40-60 %. The recorded PIV images provide information on the formation, growth, motion and break-up of clusters. The gas-solid two-phase flow in the riser has been simulated with a 3D, hard sphere, discrete particle model, applying a sub-grid scale (SGS) model to account for the influence of the gas-phase turbulence using the model recently proposed by Vreman [1]. Simulations were performed with a fixed solids influx at the bottom, which allowed investigation of the developing flow regime. The movement and patterns of the clusters and the corresponding mean and RMS particle velocities obtained from the simulations for different superficial gas velocities and solids fluxes were compared with the experimental findings showing reasonable agreement.

II. EXPERIMENTAL METHOD

Experimental Setup

A photograph and a schematic illustration of the experimental setup used in our work are shown in figure 1 (a) and (b) respectively. The setup is mainly composed of a riser, a gas-particle separation system and re-circulating system.

Experiments have been carried out in this setup with specific focus on the riser. The bed was illuminated by a laser sheet generated by a pulsed Nd:YAG laser. Images of the bed were recorded at various heights with the use of a high-speed digital camera. Further details of the experimental setup are listed in Table 1.

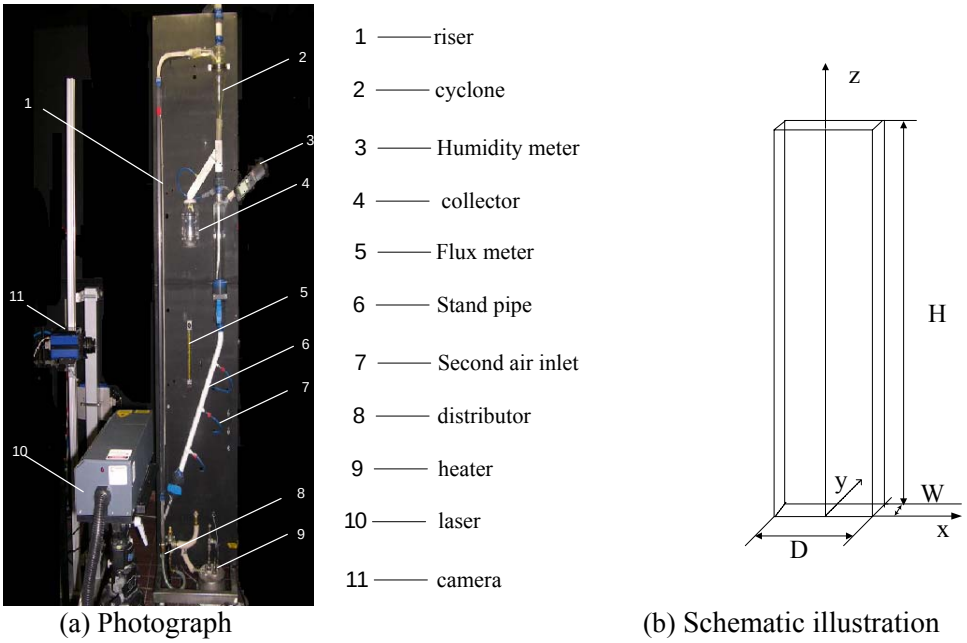

(a) Photograph (b) Schematic illustration

Figure 1 Photograph and schematic illustration of the circulating fluidized bed.

Table 1 Details of the PIV experimental setup

Camera		*Particle Properties*	
Camera	Imager Pro HS	*Particle-particle collision coefficients*	
Camera frame rate	800 Hz	Normal restitution	0.97±0.01
Pixel pitch	12 μm	Friction	0.10±0.01
Applied camera resolution	1280×581 pixels^2	Tangential restitution	0.33±0.01
		Particle-wall collision coefficients	
		Normal restitution	0.97±0.01
		Friction	0.10±0.01
		Tangential restitution	0.33±0.01

Particle velocity measurements

Particle image velocimetry (PIV) is a non-intrusive technique for the measurement of an instantaneous velocity field in one plane of a flow. In traditional PIV the flow is visualized by seeding it with small tracer particles that perfectly follow the flow. In gas-particle flows, the discrete particles can readily be distinguished, so no additional tracer particles are needed to visualize the particle movement. The flow near the front wall of the bed is illuminated with the use of a laser light sheet. A CCD camera is used to record images of the particles in the illuminated plane. Two subsequent images of the flow, separated by a short time delay, Δt, are divided into small interrogation areas. Cross-correlation analysis is used to determine the volume-averaged displacement, $\mathbf{s}_p(\mathbf{x}, t)$, of the particle images between the interrogation areas in the first and second image. The cross-correlation analysis yields a dominant correlation peak embedded in a background of noise peaks, where the location of the tallest peak corresponds to the local average particle displacement. The average particle velocity is then straightforwardly calculated from the displacement vector and the time delay between the two images.

It is difficult to get good quality images for PIV analysis in circulating fluidized beds with increasing particle volume fractions, because the laser cannot penetrate dense zones of particles. Based on visual observations, we can guarantee the right half part of the riser to be well illuminated. For this reason, only results for the right half of the bed are shown in this paper.

III. NUMERICAL METHOD

The gas flow is modeled by the volume-averaged Navier-Stokes equations:

$$\frac{\partial(\varepsilon_g \rho_g)}{\partial t} + \nabla \cdot (\varepsilon_g \rho_g \mathbf{u}_g) = 0 \tag{1}$$

$$\frac{\partial(\varepsilon_g \rho_g \mathbf{u}_g)}{\partial t} + \nabla \cdot (\varepsilon_g \rho_g \mathbf{u}_g \mathbf{u}_g) = -\varepsilon_g \nabla P - \mathbf{S}_p - \nabla \cdot (\varepsilon_g \boldsymbol{\tau}_g) + \varepsilon_g \rho_g \mathbf{g} \tag{2}$$

Here, ε_g is the porosity, and ρ_g, $\mathbf{u}_g$, τ_g and P are the density, velocity, viscous stress tensor, and pressure of the gas phase, respectively. The source term $\mathbf{S}_p$ is defined as:

$$\mathbf{S}_p = \frac{1}{V} \int \sum_{a=0}^{Npart} \frac{\beta V_a}{1-\varepsilon_g} (\mathbf{u}_g - \mathbf{v}_a) \delta(\mathbf{r} - \mathbf{r}_a) dV \tag{3}$$

Here V is the volume of the fluid cell, V_a the volume of particle, $\mathbf{v}_a$ the particle velocity, and N_{part} the number of particles. The δ-function ensures that the drag force acts as a point force at the position of the particle. To calculate the interphase momentum exchange coefficient β, we employed the well-known Ergun equation for porosities lower than 0.8 and Wen and Yu correlation for porosities higher than 0.8 [13].

$$\beta = \begin{cases} 150 \dfrac{\mu_g \varepsilon_s^2}{\varepsilon_g^2 d_p^2} + 1.75 \dfrac{\rho_g \varepsilon_s}{\varepsilon_g d_p} \left| \mathbf{u}_g - \mathbf{v}_s \right| & \varepsilon_g \le 0.8 \\ \dfrac{3 C_d \varepsilon_s \varepsilon_g \rho_g \left| \mathbf{u}_g - \mathbf{v}_s \right|}{4 d_p} \varepsilon_g^{-2.65} & \varepsilon_g > 0.8 \end{cases} \tag{4}$$

with

$$\mathrm{Re}_p = \frac{\rho_g \left|\mathbf{u}_g - \mathbf{v}_s\right| d_p}{\mu_g} \tag{5}$$

$$C_d = \begin{cases} \dfrac{24}{\mathrm{Re}}(1 + 1.15\,\mathrm{Re}^{0.687}) & \mathrm{Re} < 1000 \\ 0.44 & \mathrm{Re} \geq 1000 \end{cases} \tag{6}$$

Here Re_p, d_p, $\mathbf{v}_s$ and ε_s are the Reynolds number, diameter and velocity of the particle. ε_s and $\mathrm{C_d}$ are the solids volume fraction and the drag coefficient respectively.

The eddy viscosity of the gas is calculated by the SGS model of Vreman [1]:

$$\nu_e = c\sqrt{\frac{B_\beta}{\alpha_{ij}\alpha_{ij}}} \tag{7}$$

with

$$\alpha_{ij} = \frac{\partial \overline{u}_{g,j}}{\partial x_j} \tag{8}$$

$$\beta_{ij} = \Delta_m^2 \alpha_{mi}\alpha_{mj} \tag{9}$$

$$B_\beta = \beta_{11}\beta_{22} - \beta_{12}^2 + \beta_{11}\beta_{33} - \beta_{13}^2 + \beta_{22}\beta_{33} - \beta_{23}^2 \tag{10}$$

Here ν_e is the eddy viscosity of the gas phase. c and Δ_m are a model constant and the local filter width, which will be explained later. The symbol α stands for the (3 × 3) matrix of derivatives of the filtered velocity $\overline{u}_g$. We define that when $\alpha_{ij}\alpha_{ij} = 0$, it follows that $\nu_e = 0$. B_β is an invariant of the matrix B.

The model constant c is related to the Smagorinsky constant C_s by $c \approx 2.5C_S^2$. In our simulation we let $C_s = 0.17$ (i.e. $c \approx 2.5C_S^2 = 0.10$). This turbulence model is easily incorporated in theDPM, since it only requires the local filter width and the first-order derivatives of the velocity field.

The gas phase equations are solved numerically with a finite differencing technique, in which a staggered grid was employed to ensure numerical stability.

The discrete particle model used in this work is based on the hard-sphere model developed firstly by Hoomans [14]. In the hard sphere model the particles are assumed to be rigid spheres. Collisions are treated as binary, instantaneous, impulsive events. The restitution and friction coefficients were kept constant in the simulations.

The velocity of every individual particle can be calculated from Newton's second law, containing forces due to the pressure gradient, drag and gravitation:

$$\frac{m_a d^2\mathbf{r}_a}{dt^2} = \frac{V_a\beta}{1-\varepsilon}\left(\mathbf{u} - \mathbf{v}_a\right) - V_a\nabla P + m_a\mathbf{g} \tag{11}$$

$$I_a\boldsymbol{\Omega}_a = I_a\frac{d\boldsymbol{\omega}_a}{dt} = \mathbf{T}_a \tag{12}$$

Here, m_a is the mass of the particle, $\mathbf{T}_a$ the torque, I_a the moment of inertia, $\boldsymbol{\Omega}_a$ the rotational acceleration, and $\boldsymbol{\omega}_a$ the rotational velocity.

Initial and Boundary Conditions:

A sketch of the fluidized bed riser used in this study is shown in Figure 1(b). The simulations are carried out only for the central part of the riser section without considering inlet and exit effects. Particles are introduced into the bed with a constant solid flux through the bottom of the bed. All particles are re-distributed in the course of the simulation due to the forces acting on them. Gas is injected at the bottom of the riser. A no-slip condition is used for the gas phase at the walls. A pressure boundary condition is used for the gas phase at the top of the bed. Most of the physical parameters are chosen to correspond with the experimental settings. A smaller height of the channel was selected for the simulations compared to the experimental setup to decrease the computation times and the total number of particles was reduced accordingly. The simulation settings are summarized in Table 2. The simulation was run for 10 s and time averages were calculated during the last 5 s.

Table 2 Parameters used in the basic case

Parameter	*Value*	*Unit*
Particle diameter, d_p	335	(μm)
Solid flux, G_s	5, 10, 20	(kg/m^{2}s)
Particle density, ρ_p	2500	(kg/m^3)
Normal restitution coefficient, e_n	0.97	(-)
Tangential restitution coefficient, e_t	0.33	(-)
Friction coefficient, μ_f	0.10	(-)
CFD time step, Δt	5.0×10^{-5}	(s)
Particle time step, Δt	5.0×10^{-5}	(s)
Channel length, D	0.05	(m)
Channel width, W	0.015	(m)
Channel height, H	0.30	(m)
CFD grid number, Nx	25	(-)
CFD grid number, Ny	10	(-)
CFD grid number, Nz	60	(-)
Shear viscosity of gas, μ	1.8×10^{-5}	(Pa s)
Gas temperature, T	313	(K)
Pressure, P	1.2×10^5	(Pa)
Velocity, u_g	2.0 and 2.3	(m/s)
Particle terminal velocity, u_t	2.7	(m/s)
Number of particles, *Npart*	168,000	(-)

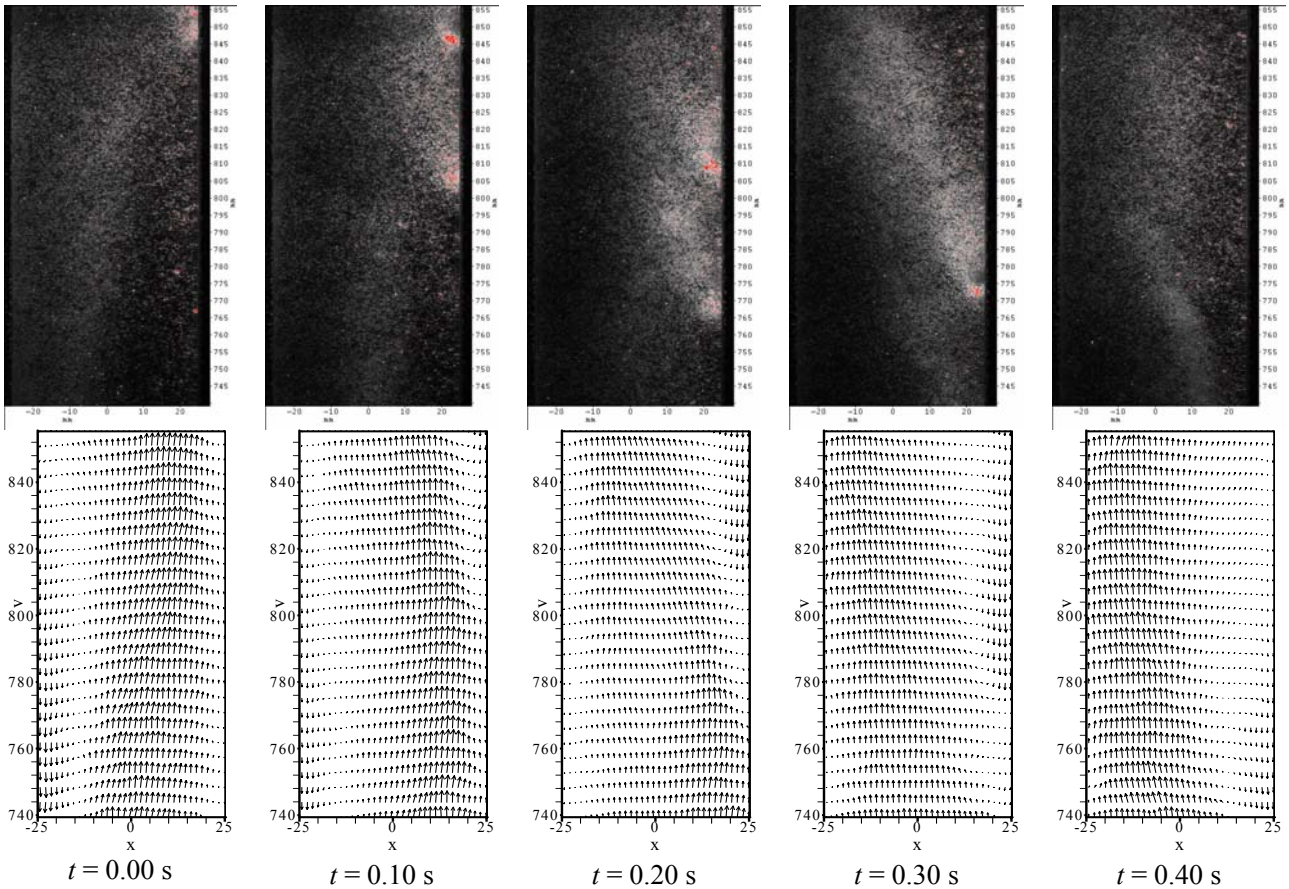

Figure 2 Snapshots of the instantaneous particle positions (top) and corresponding particle velocity fields (bottom) at a superficial gas velocity of 2.3 m/s (h = 0.740 - 0.855 m, G_s = 10 kg/m^{2}s).

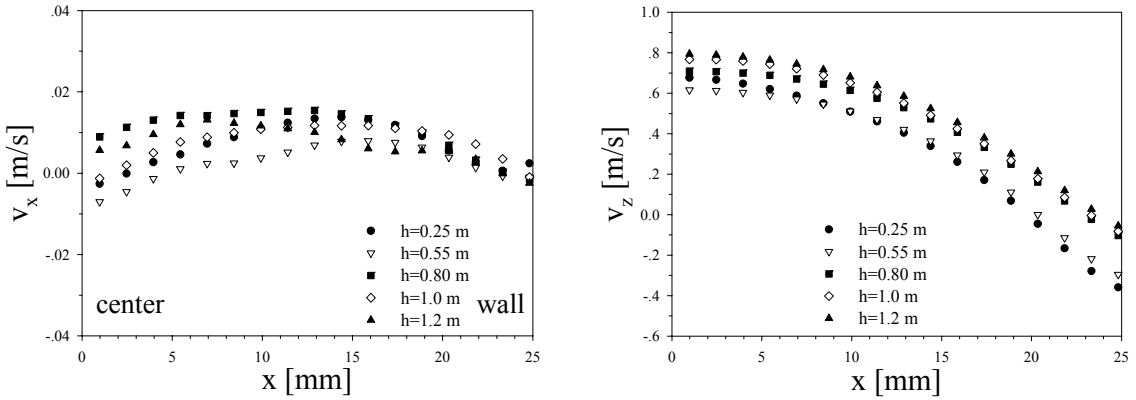

Figure 3 Average particle velocity distributions at a superficial gas velocity of 2.3 m/s at various bed heights (G_s = 10 kg/m^{2}s).

IV. RESULTS

Particle image velocimetry measurements were performed in the riser for a period of 50 s. Figure 2 shows recorded images and associated velocity fields that were obtained at a solid flux of 10 kg/m^{2}s and a superficial gas velocity of 2.3 m/s. In this figure, the movement of the clusters can very clearly be observed. The clusters move downward fast along the right wall.

It can also be observed that the particles move upward in the center of the bed, while particles move down in the proximity of the wall. When a cluster is passing by, the particles are dragged down at a higher velocity. This implies that the clusters are too heavy to be dragged by gas phase and change the flow pattern in the riser. Combined with figure 4 it can be easily seen that a cluster is followed by a wake, in which particles move downwards quickly.

Figure 3 presents the average particle velocity distributions with a solid flux of 10 kg/m^{2}s at a superficial gas velocity of 2.3 m/s at various bed heights. The radial particle velocities are very low and the majority of the particles move away from the central axis. On average the particles move downwards along the wall and move upwards in the center of the bed. From Figure 3 we can find that the vertical particle velocity profiles hardly change from a height of 0.8 m, indicating that the flow can be considered to be fully developed above this height. At a height between 0.55 m and 0.25 m the flow is still developing with the particles accelerating and acquiring more energy.

Figure 4 shows the RMS particle velocity distributions with the solid flux of 10 kg/m^{2}s at a superficial gas velocity of 2.3 m/s at various bed heights. The radial component of the RMS velocity is larger in the center of the bed and decreases towards the walls. The radial RMS particle velocities at various bed heights are nearly the same. The vertical RMS particle velocities are opposite to the radial RMS particles velocities, i.e. low in the bed center and increasing towards the walls. Close to the wall a decrease of the vertical RMS particle velocities is observed. It is noted that the vertical velocity fluctuations are considerably larger than the horizontal fluctuations, which is in accordance with the flow direction in the riser.

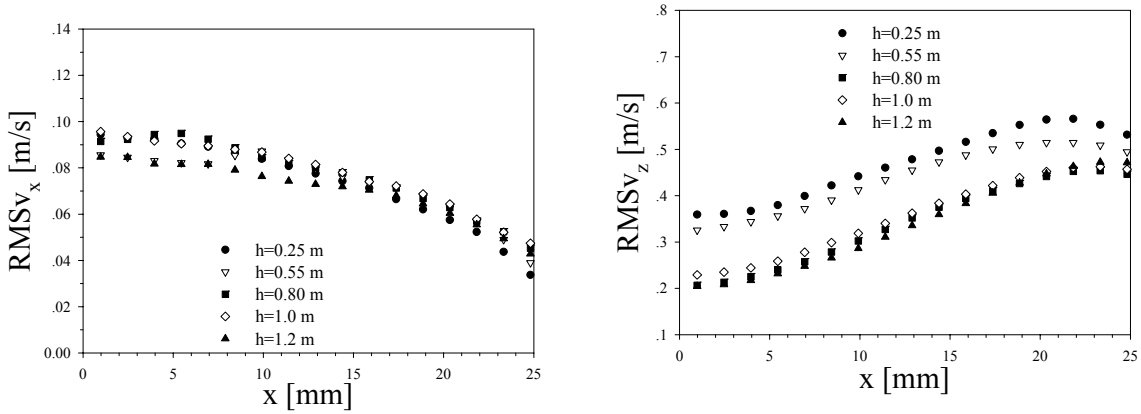

Figure 4 RMS particle velocity distributions at superficial gas velocity of 2.3 m/s at various bed heights (Gs=10 kg/m^{2}s).

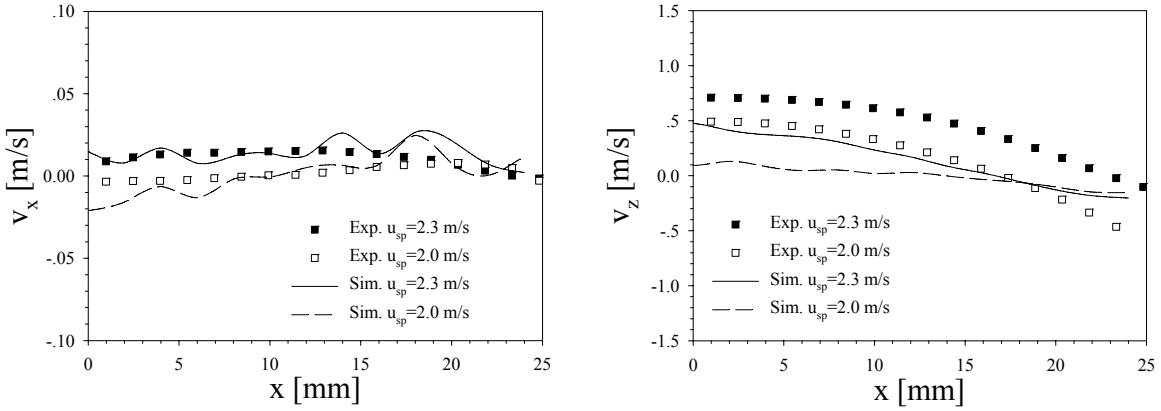

Figure 5 Average particle velocity distributions at various superficial gas velocities (h=0.80 m, Gs=10 kg/m^{2}s).

The local maximum in the vertical velocity fluctuations corresponds to the region containing most of the clusters. In the region close to the wall the fluctuations are dampened by the wall. Furthermore, it is observed that the vertical RMS particle velocity is high in the bottom of the bed and decreases with the bed height. When the height of the bed is over 0.8 m the vertical RMS particle velocities keep almost constant. As observed before, the flow is fully developed above bed heights of 0.8m. Hence the intensity of fluctuation of the particles remains nearly the same.

Because the superficial gas velocity has an important influence on the flow in a circulating fluidized bed riser, experiments at two different superficial gas velocities were performed in this work. The average particle velocity distribution at superficial gas velocities of 2.0 m/s and 2.3 m/s are shown in Figure 5. The radial velocities are small and increase slightly with increasing superficial gas velocity. The vertical velocities are high in the bed center and decrease along the radial direction. The vertical particle velocity is largest at a superficial gas velocity of 2.3 m/s. The profiles of the vertical particle velocity are nearly the same in both cases, which indicates that the superficial gas velocity has a strong influence on the axial solid velocity, and subsequently on the extent of solids down flow. Numerical results are also shown in Figure 5 with a reasonable agreement with the experimental results.

RMS particle velocities at various superficial gas velocities are shown in Figure 6. The radial RMS particle velocities are small in both cases. The vertical RMS velocities for both cases are lower in the bed center and increase with the radial direction of the bed to a peak value, and then decrease very close to the wall. The vertical RMS velocity for low superficial gas velocity changes less with the radial direction of the bed than for high superficial gas velocity. The reason for this is that the particles are less influenced by the gas phase at the lower superficial gas velocity.

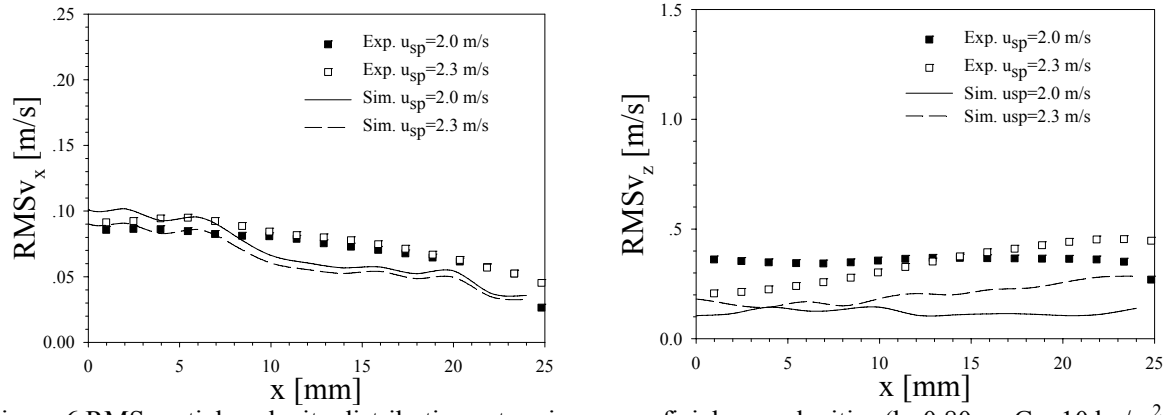

Figure 6 RMS particle velocity distributions at various superficial gas velocities (h=0.80 m, Gs=10 kg/m^{2}s).

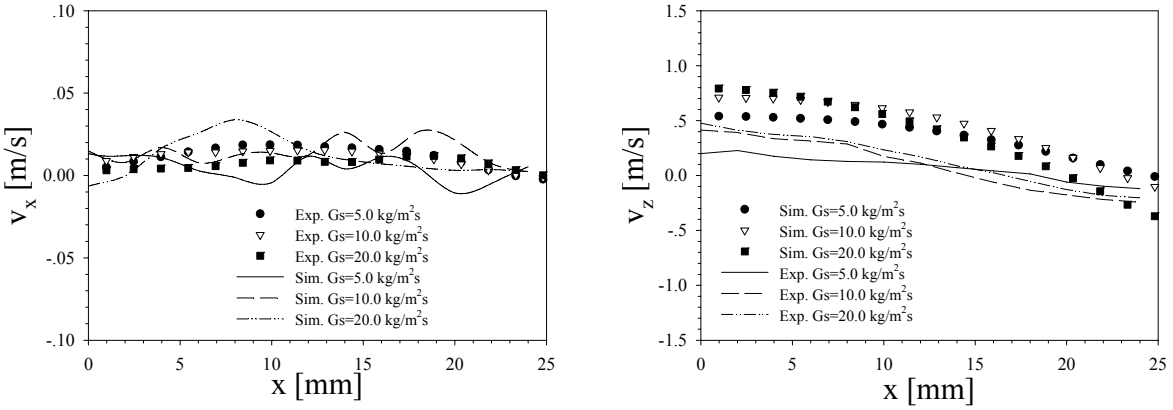

Figure 7 Average particle velocity distributions with various solid fluxes (h=0.8 m, u_{sp}=2.3 m/s).

Figure 7 shows the average particle velocity distributions with various solid fluxes at a superficial gas velocity of 2.3 m/s. The radial velocities of particles are small. The vertical velocities of particles are large in the bed center and decrease with the radial direction of the bed. The velocity profiles are steeper at higher solid fluxes. The reason for this may be that the clusters increase in size and weight at higher solid fluxes. Experimental results are compared with numerical results in Figure 7 and are found to be in reasonable agreement, showing the same trends.

RMS velocities of particles for various solid fluxes are given in Figure 8. The radial RMS velocities are nearly the same for all cases. The profiles of the vertical RMS velocities show considerable differences, which is caused by the clusters characteristics, being bigger and heavier in the case of higher solid fluxes. Further study on the cluster characteristics is necessary to explain the complex phenomena of the flow in a riser.

V. CONCLUSIONS

In this work the hydrodynamics of gas-solid two-phase turbulent flow in a riser has been studied by detailed experiments using a non-intrusive optical measurement technique, particle image velocimetry (PIV). The gas-solid two-phase flow in the riser has also been simulated with a 3D, hard sphere, discrete particle model, applying a SGS model proposed by Vreman [1] to account for the influence of gas-phase turbulence.

Experimental and numerical results show that from 0.8 m above the bottom distributor plate the core-annulus flow structure has become fully developed. It was found that the superficial gas velocity has a strong influence on the axial solids velocity, and subsequently on the extent of solids down flow. The solids flux has a large effect on the extent of solids down flow, but only little influence on the lateral profile of the RMS axial solids velocity. Experimental results in this work indicate that PIV can be an efficient tool for quantitative flow visualization in flat circulating fluidized bed, even at the relatively high particle volume fractions encountered in these systems.

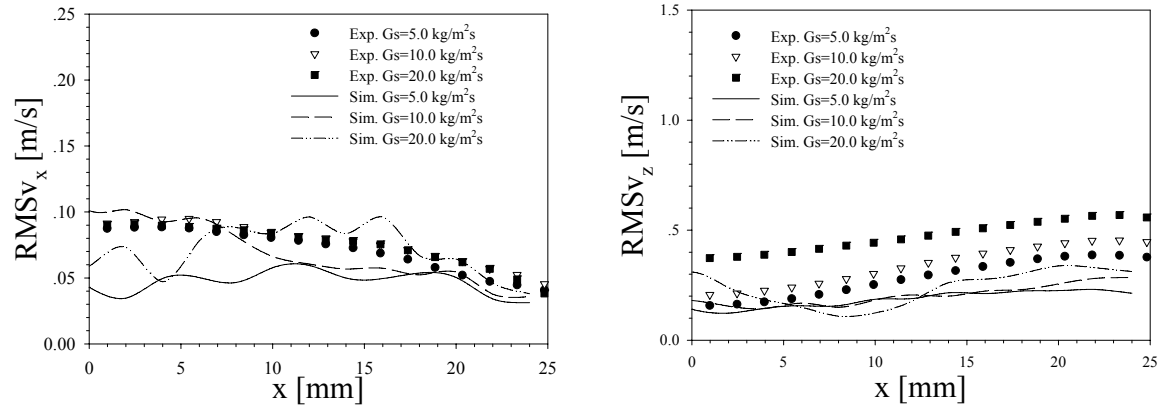

Figure 8 RMS particle velocity distributions with various solid fluxes (h=0.8 m, u_{sp}=2.3 m/s).

VI. ACKNOWLEDGEMENTS

This work was supported by the National Science Foundation through Grant No. 50376013 and NSFC-PetroChina Company Limited under the cooperative project No. 20490200.

VII. REFERENCES

[1] Vreman, A.W., An Eddy-viscosity Subgrid-scale Model for Turbulent Shear Flow: Algebraic Theory and Applications. Phys. Fluids 16 (2004) 3670-3681.
[2] Mathiesen, V., Solberg, T., Arastoopour, H., Hjertager, B.H., Experimental and computational study of multiphase gas/particle flow in a CFB riser. AIChE J. 45 (1999) 2503–2518.
[3] Neri, A., Gidaspow, D., Riser hydrodynamics: simulation using kinetic theory, AIChE J. 46 (2000) 52-67.
[4] Parssinen J. H., Zhu J.X., Axial and radial solids distribution in a long and high-flux CFB riser, AIChE J. 47 (2001) 2197-2205.
[5] Harris A.T., Davidson J.F., Thorpe R.B., Influence of exit geometry in circulating fluidized-bed risers, AIChE J. 49 (2003) 52-64.
[6] Wang, X., Gao, S., Xu, Y., Zhang, J., Gas-solid flow patterns in a novel dual-loop FCC riser, Powder Technology 152 (2005) 90-99.
[7] Sinclair J.L., Jackson R., Gas-particle flow in a vertical pipe with particle–particle interactions. AIChE J. 35 (1989) 1473-1486.
[8] Nieuwland, J.J., Van Sint Annaland, M., Kuipers, J.A.M., Van Swaaij, W.P.M., Hydrodynamic modeling of gas-particle flows in riser reactors, AIChE J. 42 (1996) 1569-1582.
[9] Hrenya, C.M., Sinclair, J.L., Effects of particle–particle turbulence in gas–solids flows, AIChE J. 43 (1997) 853-871.
[10] Lu, H., Gidaspow, D., Hydrodynamics of binary fluidization in a riser: CFD simulation using two granular temperature, Chemical Engineering Science 58 (2003) 3777-3792.
[11] Tsuji, Y., Tanaka, T., Yonemura, S., Cluster patterns in circulating fluidized beds predicted by numerical simulation (discrete particle model versus two-fluid model). Powder Technology 95 (1998) 254-264.
[12] Sun, Q., Lu, H., Liu, W., He, Y., Yang, L., Gidaspow, D., Simulation and experiment of segregating/mixing of rice husk–sand mixture in a bubbling fluidized bed, Fuel 84 (2005) 1739-1748.
[13] Gidaspow, D., Multiphase Flow and Fluidization. Continuum and Kinetic Theory Description. Academic Press, New York, 1994.
[14] Hoomans, B.P.B., Granular Dynamics of Gas-solid Two-phase Flows. Ph.D. Thesis, University of Twente, 2000.